2487 (1994)] demonstrated that the rate-controlling flow process in H-D creep is the climb of dislocations saturated with vacancies. The incorporation of water into quartz structure enhances the concentration of O or Si vacancies, depending on the neutrality condition [B. E. Hobbs, in *Point Defects in Minerals*, R. N. Schock, Ed. (American Geophysical Union, Washington, DC, 1985), pp. 151–170]. Thus, dislocations might be saturated in the gel-origin quartzite with high water concentrations (> 5500 H per 10^6 Si) but might not be saturated in the silicic acid–origin quartzite, which has low water concentrations (generally much lower than 4500 H per 10^6 Si).

11. P. S. Koch, J. M. Christie, A. Ord, R. P. George Jr., *J. Geophys. Res.* **94**, 13975 (1989); A. K. Kronenberg and J. Tullis, *ibid.* **89**, 4281 (1984); O. Jaoul, J. Tullis, A. K. Kronenberg, *ibid.*, p. 4298.
12. F. A. Mohamed and T. J. Ginter [*Acta Metall.* **30**, 1869 (1982)] showed that H-D creep would not be observed in Al specimens unless the dislocation density in the sample before loading was sufficiently low. This result indicates that there might be a substructural requirement for the occurrence of H-D creep.
13. J. N. Wang, *Scr. Metall.* **29**, 733 (1993); *ibid.*, p. 1505; *Philos. Mag. A*, in press.
14. _____ and M. Toriumi, *Mater. Sci. Eng.*, in press.
15. M. S. Paterson and F. C. Luan, in *Deformation Mechanisms, Rheology, and Tectonophysics*, R. J. Knipe and E. H. Rutter, Eds. (Geological Society Special Publication 54, London, 1990), pp. 299–307.
16. Postdoctoral support for J.N.W. was provided by the Japan Society for the Promotion of Science. J. N. W. thanks J. N. Boland for instructing some TEM work and many people (especially S. He) in Central South University of Technology, Changsha, for valuable discussion. Comments by J. Tullis improved the report.

11 January 1994; accepted 29 June 1994

The Nature of the Glass Transition in a Silica-Rich Oxide Melt

Ian Farnan* and Jonathan F. Stebbins†

The atomic-scale dynamics of the glass-to-liquid transition are, in general, poorly understood in inorganic materials. Here, two-dimensional magic angle spinning nuclear magnetic resonance spectra collected just above the glass transition of $K_2Si_4O_9$ at temperatures as high as 583°C are presented. Rates of exchange for silicon among silicate species, which involves Si–O bond breaking, have been measured and are shown to be closely related in time scale to those defined by viscosity. Thus, even at viscosities as high as 10^{10} pascal seconds, local bond breaking (in contrast to the cooperative motion of large clusters) is of major importance in the control of macroscopic flow and diffusion.

Molten silicates play a major role in heat and mass transfer in the crust and mantle of the Earth, as well as being the precursors to technological materials such as glass and ceramics. If crystal nucleation and growth rates are slow in comparison to the rate of temperature decrease, cooling of a silicate liquid will result in its transformation to a glass at a rate-dependent temperature T_g. This transition is generally marked by substantial decreases in heat capacity, thermal expansivity, and compressibility that reach values in the glass that are similar to those of the corresponding crystalline solid. The glass transition is traditionally viewed as the temperature at which the rate of change of the structure of the liquid with cooling (α structural relaxation) becomes too slow to remain in equilibrium at the given cooling rate. More rapid β processes, while of relatively minor bulk energetic consequence in silicates, may contribute to ultrasonic and dielectric relaxation both above and even well below T_g (*1*). The uncoupling of α processes from β processes during cooling may be an important part of the transition from liquid to glass (*2*).

The configurational entropy generated by structural change above T_g is quantitatively linked to viscosity (*3*). An understanding of the structural mechanism of the transition to a glass can thus provide insights into both thermodynamic and transport properties of the liquids, as well as the relaxation that takes place during annealing of glasses, which transforms them into usable materials. In this report, we describe two-dimensional (2D) ^{29}Si magic angle spinning nuclear magnetic resonance (MAS-NMR) experiments on $K_2Si_4O_9$ liquid at temperatures just above T_g that provide a new quantitative link between bulk viscosity and a microscopic mechanism of exchange among structural species.

As a liquid, $K_2Si_4O_9$ consists of a network of SiO_4 tetrahedra, with some relatively large sites occupied by network-modifying K^+ cations. In about half of the tetrahedra (Q^4 groups), all four oxygens are linked to other tetrahedra (bridging oxygens); in the other half (Q^3 species), one oxygen is not shared by a second Si but is coordinated by several K^+ cations (nonbridging oxygens). A variety of minor species are also present, including SiO_5 groups (*4*). At normal laboratory cooling rates, T_g for this liquid is close to 500°C (*5*). In previous one-dimensional (1D) static (non-MAS) ^{29}Si NMR work at higher temperatures (*6*), the presence of a single resonance line indicated rapid chemical exchange of silicon between Q^3 and Q^4 groups. The measured rates at which these species exchange with each other, and also the rate at which bridging and nonbridging oxygens exchange, was used in a simple model to accurately predict the bulk viscosity down to about 850°C (*6*, *7*).

A possible mechanism for this process, which is consistent with a number of published molecular dynamics simulations, is shown in Fig. 1. At these higher temperatures this two-step exchange process passes easily through the intermediate step to complete exchange from Q^3 to Q^4. The NMR exchange rate data could also be collected down to 690°C, but in this lower range, predicted viscosities were significantly lower than experimental values. This divergence is probably a result of the progressive inhibition of complete exchange and the increased importance of self-exchange to 1D NMR line narrowing. Formation of the intermediate state (Fig. 1) followed by decay back to original Q^3 and Q^4 species without exchange but with changed orientations with respect to the external magnetic field will contribute to 1D NMR peak narrowing but not to the flow mechanism of the liquid because there is no net throughgoing motion of an oxide anion. The 1D NMR spectra are limited because they are sensitive only to motions with frequencies within about an order of magnitude of the frequency separation and widths (in hertz) of their component peaks. For the static ^{29}Si NMR spectrum of $K_2Si_4O_9$, this is ~10 kHz, and the slowest motions that could be detected were thus about 1 kHz.

In contrast, 2D chemical exchange NMR experiments can detect much slower motions and can also separate the complete exchange from other peak-narrowing processes. This approach has been developed and elegantly applied to quantify dynamics in organic polymers, including studies of the nature of the glass transition (*8*,*9*). The technique has been described in detail (*10*) and involves a typical 2D NMR sequence of preparation, evolution, mixing, and detection. The 2D Fourier transform produced at the end of the experiment displays correlations between the NMR frequency of a nucleus at the start and at the end of the mixing time. The mixing time (t_{mix}) is chosen to probe characteristic times associated with exchange in the sample, and observable dynamics are thus not limited by

Department of Geological and Environmental Sciences, Stanford University, Stanford, CA 94305, USA.

*Present address: Centre de Recherches sur la Physique des Hautes Températures, Conseil National de Recherche Scientifique, 45071 Orléans Cedex 2, France.
†To whom correspondence should be addressed.

the width or frequency separation of lines. In the event of no exchange, a nucleus will retain the same frequency throughout t_{mix}, and all intensity in the 2D spectrum will be along the diagonal (with the two frequencies $\omega_1 = \omega_2$). Nuclei that exchange from one local environment to a different one can be identified by off-diagonal cross peaks. The intensity of the off-diagonal peaks can also be analyzed as a function of mixing time to estimate the exchange rate. In our previous static 2D NMR study, we were able to collect data at 571°C for a single mixing time of 500 ms in which considerable exchange took place (*11*). This was similar to the shear relaxation time of 300 ms estimated from viscosity data (see below).

We have now considerably refined this study by using MAS-NMR, which recently has become possible at temperatures at high as 600°C (*12–14*). The much higher resolution obtainable in MAS experiments allows more rapid data collection than with nonspinning samples and permits much slower exchange to be observed. We have therefore been able to collect data with a range of mixing times at several temperatures and have increased by about an order of magnitude the time scale of exchange that can be observed, allowing dynamics closer to T_g to be quantified (*15*).

A 1D MAS spectrum for $K_2Si_4O_9$ liquid at 555°C (Fig. 2) is nearly identical to ambient temperature spectra (*4*). Peaks for Q^3 and Q^4 sites are clearly resolved. The lack of any indication of exchange places an initial upper limit of ~70 Hz on the exchange frequency because the peak separation is ~700 Hz. In the 2D spectrum with a t_{mix} of 500 ms (Fig. 3A), off-diagonal intensity is low. This lowers the maximum exchange frequency of silicons between Q^3 and Q^4 environments to less than ~2 Hz [1/(500 ms)]. However, when t_{mix} is lengthened to 4 s (Fig. 3B), off-diagonal intensity increases markedly, although resolution is poor because of ranges in chemical shift for each species (self-exchange that results in changes in bond angles or distances at a given site could also lead to broadening). The effect of exchange among different species can be most clearly seen in 1D slices through the 2D spectrum taken at the position of the main Q^4 peak (Fig. 4). Again with t_{mix} = 500 ms, only the broad Q^4 peak, centered at a frequency shift of about −105 parts per million (ppm) is visible. With longer values of t_{mix}, a distinct second peak appears at −95 ppm, corresponding to the Q^3 position in the 1D spectrum. By plotting the relative peak intensities versus t_{mix}, we estimate an average exchange time of about 3 ± 2 s for Q^3 to Q^4 exchange (*16*). The near equality of the intensities of the Q^4 and the exchange peak in the slice for the longest mixing time indicates that exchange is essentially complete, that is, that most or all Q^4 sites participate in exchange. The quality of the spectra obtainable at this time only permits an average exchange time to be determined. We are not yet able to determine the breadth of the distribution of exchange times that must be present in a liquid that has considerable static and dynamic disorder.

At 583°C, a sample spinning rate of only about 2.0 kHz was obtainable, leading to considerable intensity in spinning sideband peaks. In this case, the most obvious exchange was between the central Q^4 peak and the first Q^3 side band. Again, by analyzing 1D slices of the 2D spectrum through the Q^4 position, we estimate the exchange time to be 0.3 ± 0.2 s. No exchange was detectable below T_g even at long mixing times, indicating that Q^3-Q^4 exchange does indeed "freeze out" at the glass transition and that spin diffusion is not the cause of the observed off-diagonal intensity.

Several approaches can be taken to relate the time scale for a microscopic flow event to that of macroscopic transport. As in previous studies (*7*), a simple Eyring model can relate viscous flow to the jumping of a single species from one site to another with a characteristic time τ, distance d, and absolute temperature T, with viscosity $\eta = 2k_BT\tau/d^3$, where k_B is Boltzmann's constant (Fig. 5) (*17*). Alternative-

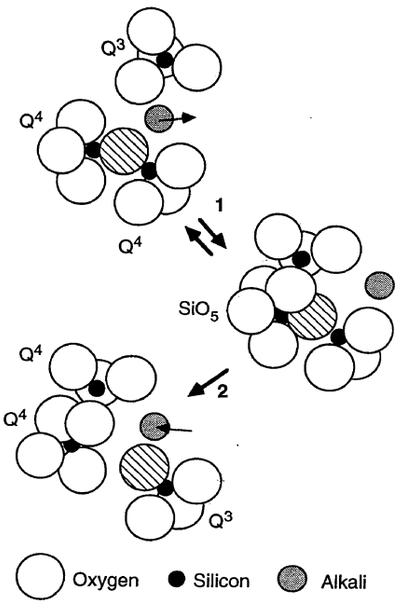

Fig. 1. Sketch of a possible mechanism for the exchange of silicon environments in a high silica liquid. Oxygens are shown as open circles, network modifying cations as shaded circles, and silicon cations as dark circles. In step 1, a nonbridging oxygen in a Q^3 group approaches a Q^4 unit as the modifier cation moves away, and a silicon originally in a Q^4 site becomes 5-coordinated. Perhaps depending on additional modifier cation motion, this SiO_5 transition complex then decays back to a Q^4, either reforming the original configuration (self-exchange) or proceeding by means of step 2 to form a new Q^3 site in a completed exchange event. Only the latter contributes to macroscopic flow, and at low temperatures at least, it is much less frequent than the reversal of step 1.

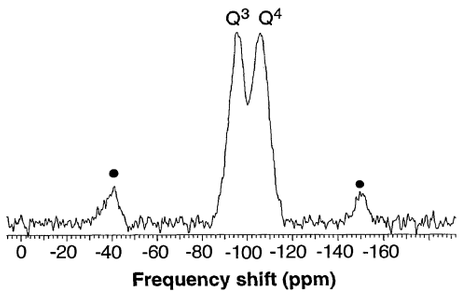

Fig. 2. A 1D ^{29}Si MAS NMR spectrum of $K_2Si_4O_9$ liquid at 555°C spinning at 4060 Hz, with 100 2-μs (π/10) pulses and a 3-s delay. Frequency shifts, in parts per million (ppm), are referenced to tetramethylsilane at room temperature. Solid circles mark spinning side bands.

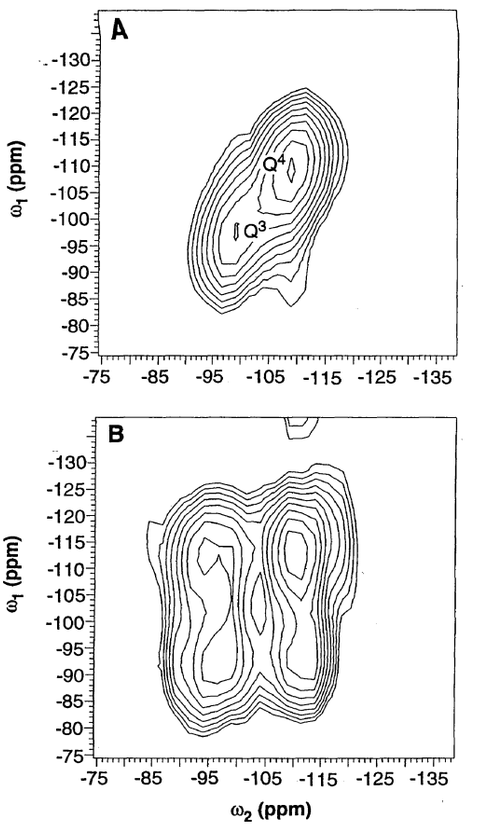

Fig. 3. A 2D ^{29}Si chemical exchange NMR spectra of $K_2Si_4O_9$ liquid at 555°C. Mixing time (**A**) t_{mix} = 0.5 s and (**B**) t_{mix} = 4.0 s. The spinning rate was 4060 Hz, with π/2 pulses of 10.5 μs and a recycle delay of 120 s. Two free induction decays were added per t_1 increment, and the t_1 dimension was zero-filled to 512 points to make a 512 × 512 data matrix.

ly, the Stokes-Einstein equation can be used to link viscosity to diffusivity, with $\eta = k_B T\tau/(3\pi a d^2)$, where a is an ionic radius (6). Both predict viscosities close to the measured values, with the latter having the better agreement. Thus, it is clear that even at only 55°C above the glass transition ($T/T_g = 1.07$), local species exchange is closely related to macroscopic viscous flow (*18*).

A more thermodynamic approach can be taken if a relaxation time is calculated as the ratio of the viscosity to the infinite frequency shear modulus ($\tau_s = \eta_s/G_\infty$, with $G_\infty \approx 10^{10}$ Pa). This relation has been shown to accurately relate at least the mean, macroscopic τ_s for enthalpic or volumetric relaxation to η (*19*). The quantity τ_s has been equated with a characteristic time for microscopic flow events, as well (*20, 21*), and can thus be directly compared with exchange times derived from NMR. The latter are about 0.5 to 1 log unit above (slower) than the curve predicted from measured viscosities, both at high temperatures and near T_g (Fig. 5). This suggests that the NMR may be sampling the longer time scales in a distribution of relaxation times slightly above the mean τ_s. This is not surprising given that bulk shear relaxation may involve significant structural motion over distance scales shorter than those for diffusive jumping.

The selectivity of the 2D NMR exchange experiment thus allows us to observe just the Q species exchange, independent of rotational self-exchange, and it appears to be the former process that constitutes the flow event. An extrapolation of the results from 1D NMR at higher temperatures would show an increasing divergence from the macroscopic data as temperature decreased, indicating the presence of faster motions that do not contribute to flow. These are probably related to the reverse step 1 in the mechanism proposed in Fig. 1. This apparent decoupling of the time scales for these two processes as T_g is approached is intriguingly similar to models involving the decoupling of α and β relaxation processes (*22*).

The observed silicon species exchange requires the breaking and reforming of Si–O bonds. If flow occurred through a local, nonmolecular mechanism, such as the diffusion of oxygen ions [as has been suggested by the success of the Eyring model in relating viscosity to oxygen tracer diffusion in some silicate liquids (*23*)], the close relation noted here is expected. However, other mechanisms may be implied from some models of silicate liquid structure. For example, a number of models of entropies and volumes of mixing in silicate liquids have assumed highly polymerized clusters or molecules of silica-like (mostly Q^4's) structure. The surfaces of these clusters would consist primarily of Q^3 sites, and connection among clusters would consist primarily of weak bonds between nonbridging oxygens and K^+ ions. Viscous flow could thus occur by relative motion of the clusters with little Si–O bond breaking or silicate species exchange (as in "reptation" models for flow in organic polymers). This kind of mechanism seems to be inconsistent with our results, which show a close relation between local species exchange and viscosity. Indeed, potassium silicate liquids are thought to be relatively unclustered because of the low field strength of K^+. Even in a system that can be shown by NMR relaxation time measurements to be compositionally heterogeneous at the nanometer scale ($Li_2Si_4O_9$ glass), clusters are fractal in character (*24*), probably forming an interwoven network that still requires Si–O bond breaking for flow to occur. However, in other liquids containing higher field strength cations, or in systems with lower contents of network-forming oxides, it is possible that more clustered silicate structural units could have a much longer average lifetime than the shear correlation time. A variety of silicate and aluminate liquid compositions, including some rich in Mg^{2+} and some very low in silica, have now been studied at temperatures well above T_g by high resolution static 1D NMR (*25–29*). In all of these, the spectra were fully averaged, indicating complete species exchange. These findings place only a maximum limit on the exchange times. It is clear that in high silica systems such as $K_2Si_4O_9$, the complete Q species exchange is intimately related to the mechanism of viscous flow and α structural relaxation; in fact, the exchange fits the criteria to be the α process itself. The possibility of performing high-resolution MAS-NMR experiments at temperatures above T_g for a variety of liquids much lower in SiO_2 than described here holds the potential for investigating the generality of this mechanism.

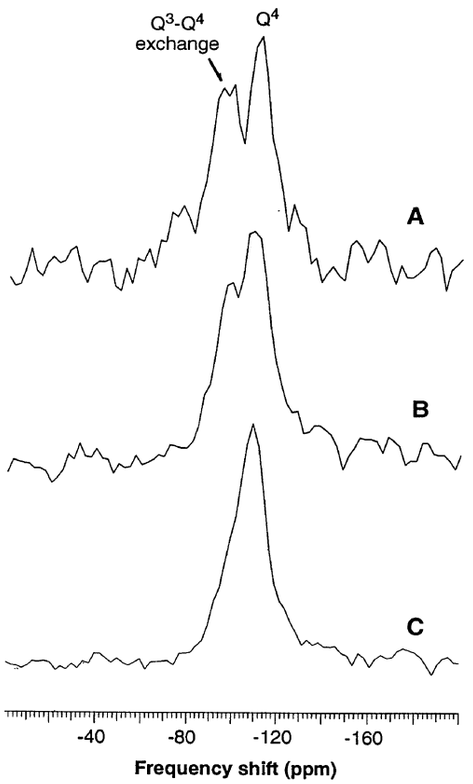

Fig. 4. Slices parallel to the ω_2 axis at the position of the Q^4 diagonal peak in 2D ^{29}Si chemical exchange NMR spectra of $K_2Si_4O_9$ liquid at 555°C for mixing times of (A) 4 s, (B) 2 s, and (C) 0.5 s. Exchange is detected by the appearance of the off-diagonal Q^3 peak (~−95 ppm) with increased mixing time. The Q^4 peak and the off-diagonal Q^4-Q^3 exchange peak are labeled.

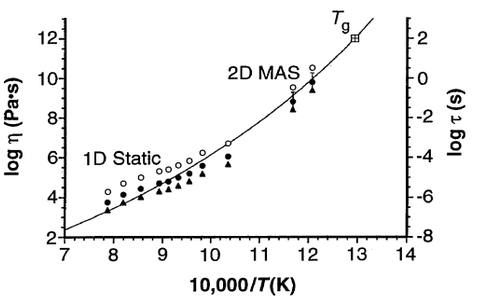

Fig. 5. Plot of $\log_{10}$ of viscosity η and $\log_{10}$ of shear relaxation time τ for $K_2Si_4O_9$ liquid versus inverse temperature. The solid curve is a fit to measurements of bulk viscosity (*17*), which can be converted to mean shear relaxation times (right-hand scale). Open circles are exchange times derived directly from the NMR spectra; solid triangles are viscosities derived from the NMR data with the Eyring equation; and solid circles are viscosities derived with the Stokes-Einstein equation (*16*). Uncertainties for the 1D points are similar in size to the symbols; for clarity, those for the 2D MAS data are shown on one pair of points only.

REFERENCES AND NOTES

1. S. Brawer, *Relaxation in Viscous Liquids and Glasses* (American Ceramic Society, Columbus, OH, 1985).
2. K. L. Ngai and R. W. Rendell, in *The Physics of Non-Crystalline Solids*, L. D. Pye, W. C. LaCourse, H. J. Stevens, Eds. (Taylor and Francis, London, 1992), p. 309.
3. P. Richet and D. R. Neuville, in *Thermodynamic Data*, S. K. Saxena, Ed. (Springer-Verlag, New York, 1992), p. 132.
4. J. F. Stebbins and P. McMillan, *J. Non-Cryst. Solids* **160**, 116 (1993).
5. J. E. Shelby, *J. Appl. Phys.* **47**, 4489 (1976).
6. I. Farnan and J. F. Stebbins, *J. Am. Chem. Soc.* **112**, 32 (1990).
7. J. F. Stebbins, I. Farnan, X. Xue, *Chem. Geol.* **96**, 371 (1992).
8. K. Schmidt-Rohr and H. W. Spiess, *Phys. Rev. Lett.* **66**, 3020 (1991).
9. S. Kaufmann, S. Wefing, D. Schaeffer, H. W. Spiess, *J. Chem. Phys.* **93**, 197 (1990).
10. J. Jeener, B. H. Meier, P. Bachmann, R. R. Ernst, *ibid.* **71**, 4546 (1979).
11. I. Farnan and J. F. Stebbins, *J. Non-Cryst. Solids* **124**, 207 (1990).

12. J. F. Stebbins, I. Farnan, E. H. Williams, J. Roux, *Phys. Chem. Miner.* **16**, 763 (1989).
13. D. R. Spearing, I. Farnan, J. F. Stebbins, *ibid.* **19**, 307 (1992).
14. D. R. Spearing, J. F. Stebbins, I. Farnan, *Am. Mineral.*, in press.
15. Spectra were collected with a modified Varian VXR400S spectrometer at a resonant frequency of 79.5 MHz for ^{29}Si and with a high-temperature MAS probe from Doty Scientific. We used 90° pulse lengths of 10.5 μs and spinning rates of 3 to 4.5 kHz. Temperatures were calibrated by spinning an empty sample container with an inserted thermocouple in the probe at high temperature. Delay times between radio-frequency pulse trains were selected after measurement of spin-lattice relaxation times to avoid saturation effects. The 2D spectra shown took 1 to 2 hours each to collect. The abundance of SiO_5 groups is too small, unfortunately, to directly test the involvement of this species in exchange (*30*). The $K_2Si_4O_9$ glass was synthesized from 95% ^{29}Si-enriched SiO_2 and K_2CO_3 as described previously (*4*) and was doped with 0.2 weight % CoO to accelerate spin-lattice relaxation.
16. Exchange rates were derived by plotting the natural logarithm of the ratios of the intensities of the exchange and Q^4 peaks in the slices shown in Fig. 4 versus mixing time. If (as is the case for this sample) spin-lattice relaxation times are long when compared to t_{mix}, the slope of this plot is equal to the exchange rate $1/\tau_{exchange}$ (*10*). The estimated uncertainties include errors in this fit as well as in intensities.
17. In calculating viscosity from the observed exchange times, we chose $d = 0.31$ nm as a typical Si-Si distance and $a = 0.04$ nm as the radius of the Si cation. For both models, the Einstein-Smoluchowski equation ($D = d^2/2\tau$) is chosen to relate diffusivity to jump time (*31*). For the Eyring model, $\eta = k_BT/(dD)$; for the Stokes-Einstein model, $\eta = k_BT/(6\pi aD)$. The simple statistical character of these equations cannot be expected to reproduce the details of a complex, partially ionic, partially covalently bonded liquid, but they are nonetheless useful starting points.
18. The solid line in Fig. 5 results from a fit to published data both at relatively high temperature (*32*) and near to T_g (*33*), with $\log \eta = -2.654 + 5069/(T - 423.4)$, with T in kelvins and η in pascal seconds. This predicts other fiber elongation rates to within 0.15 log units (*34*). We observed the glass transition behavior of our NMR sample of $K_2Si_4O_9$ directly using a Dupont 2100 differential scanning calorimeter. After cooling at 20°C/s and heating at the same rate, we recorded an onset temperature of 490° ± 2°C and a peak temperature of 534° ± 2°C. Our fit equation for viscosity predicts $\log \eta = 12.3$ and 10.6 (Pa · s) at these temperatures. A dilatometric value of T_g of 500°C, at which point $\log \eta$ is typically 12.0 (Pa · s), has been reported (*5*).
19. G. W. Scherer, *Relaxation in Glass and Composites* (Wiley, New York, 1986).
20. C. A. Angell, *J. Non-Cryst. Solids* **131–133**, 13 (1991).
21. D. B. Dingwell and S. L. Webb, *Eur. J. Mineral.* **2**, 427 (1990).
22. K. L. Ngai, R. W. Rendell, A. K. Rajagopal, S. Teitler, *Ann. N.Y. Acad. Sci.* **484**, 150 (1986).
23. N. Shimizu and I. Kushiro, *Geochim. Cosmochim. Acta* **48**, 1295 (1984).
24. S. Sen and J. F. Stebbins, *Phys. Rev. B*, in press.
25. B. T. Poe *et al.*, *J. Phys. Chem.* **96**, 8220 (1992).
26. P. Fiske and J. F. Stebbins, *Am. Mineral.*, in press.
27. J. F. Stebbins and I. Farnan, *Science* **255**, 586 (1992).
28. B. Coté, D. Massiot, F. Taulelle, J. Coutures, *Chem. Geol.* **96**, 367 (1992).
29. S. Shimokawa *et al.*, *Chem. Lett.* **1990**, 617 (1990).
30. J. F. Stebbins, *Nature* **351**, 638 (1991).
31. P. W. Atkins, *Physical Chemistry* (Freeman, New York, 1986).
32. L. Shartsis, S. Spinner, W. Capps, *J. Am. Ceram. Soc.* **35**, 155 (1952).
33. S. L. Webb and D. B. Dingwell, *Phys. Chem. Miner.* **17**, 125 (1990).
34. O. V. Mazurin, M. V. Streltsina, T. P. Shvaiko-Shvaikovskaya, *Silica Glass and Binary Silicate Glasses* (Elsevier, New York, 1983).
35. This work was supported by National Science Foundation grants EAR 8905188 and EAR 9204458. We thank the two anonymous reviewers for insightful and helpful comments.

28 April 1994; accepted 12 July 1994

Molecular Origins of Friction: The Force on Adsorbed Layers

Marek Cieplak,* Elizabeth D. Smith, Mark O. Robbins†

Simulations and perturbation theory are used to study the molecular origins of friction in an ideal model system, a layer of adsorbed molecules sliding over a substrate. These calculations reproduce several surprising features of experimental results. In most cases, the frictional force on a solid monolayer has a different form from that observed between macroscopic solids. No threshold force or static friction is needed to initiate sliding; instead, the velocity is proportional to the force. As in experiments, incommensurate solid layers actually slide more readily than fluid layers. A comparison of experiment, simulation, and analytic results shows that dissipation arises from anharmonic coupling between phonon modes and substrate-induced deformations in the adsorbate.

Friction plays a key role in holding our buildings and clothes together, determining the function and failure of our machines, and allowing us to sense the outside world. However, our understanding of the molecular origins of this force is relatively primitive. The goal of this report is to provide a detailed molecular description of friction in an ideal model system, a layer of molecules adsorbed on a solid substrate.

The frictional force between macroscopic solids is normally described by phenomenological laws. Fluid dynamics implies that the friction F for a lubricated contact is proportional to the relative velocity v of the solids. We will refer to this linear velocity dependence as "viscous" friction. The behavior of dry contacts is normally very different. A static frictional force F_{stat} must be exceeded to initiate sliding, and there is a smaller kinetic friction F_{kin} between sliding solids that is only weakly dependent on v. We will refer to this type of behavior as "static" friction.

New experimental methods have made it possible to study friction in single contacts of well-defined area. The results are often strikingly different from those expected from macroscopic laws. For example, static friction and stick-slip motion are observed in lubricated contacts when the film thickness becomes comparable to molecular dimensions (*1*, *2*). Recent simulations indicate that this unusual behavior is due to solidification of the lubricant by the confining solid walls (*3*, *4*).

Experimental studies of the frictional force between a substrate and an adsorbed monolayer also produce surprising results (*5*, *6*). Crystalline layers exhibit viscous rather than static friction laws. Indeed, crystalline monolayers slide more readily than fluid monolayers. The measured forces for both phases are smaller by roughly three orders of magnitude than expected from the bulk viscosity of the adsorbed phase. We show here that these counterintuitive results can be reproduced by simulations and perturbation theory. These calculations provide a quantitative description of the frictional force in terms of the excitation and subsequent decay of phonon modes in the adsorbed film.

Most experimental studies of the frictional force on adsorbed films have used noble gas atoms adsorbed on the (111) surfaces of noble metal substrates (Au or Ag) (*5*–*7*). The equilibrium properties of these systems have been extensively studied by researchers interested in two-dimensional phase transitions (*8*). Because the substrate is much more rigid than the adsorbate, the displacement of substrate molecules from ideal lattice sites is usually ignored. The substrate then produces a fixed periodic potential that acts on the adsorbed layer. We made this approximation in most of our calculations and discuss its limitations below.

The interactions between noble gas adsorbate atoms are well described by a Lennard-Jones potential

$$V(r) = 4\varepsilon[(\sigma/r)^{12} - (\sigma/r)^6] \qquad (1)$$

where r is the atomic separation and ε and σ are characteristic energy and length

Department of Physics and Astronomy, Johns Hopkins University, Baltimore, MD 21218, USA.

*On leave from the Institute of Physics, Polish Academy of Sciences, 02-668 Warsaw, Poland.
†To whom correspondence should be addressed.